July 2026, Volume 20, Number 3

Iranian Journal of Toxicology
ARAK UNIVERSITY OF MEDICAL SCIENCES

Research Paper

Effect of Methamphetamine on Human Spatial Arrangement in Testicular Cells

Arian Karimi Rouzbahani[1,2], Samaneh Tahmasebi Ghorabi[3], Reyhane Faghih[4], Arya Behzadi[5,6], Arefeh Aryan[7*]

[1] *Department of Urology, Western Health, Melbourne, Australia.*
[2] *Surgery Education and Researching Network (SERGN), Universal Scientific Education and Research Network (USERN), Khorramabad, Iran.*
[3] *USERN Office, Lorestan University of Medical Sciences, Khorramabad, Iran.*
[4] *Student Research Committee, Shahid Sadoughi University of Medical Sciences, Yazd, Iran.*
[5] *School of Medicine, Shahid Beheshti University of Medical Sciences, Tehran, Iran.*
[6] *Surgery Education and Researching Network (SERGN), Universal Scientific Education and Research Network (USERN), Melbourne, Australia.*
[7] *Department of Anatomical Sciences, Lorestan University of Medical Sciences, Khorramabad, Iran.*

Scan to access website

How to cite this paper:
Karimi Rouzbahani A, Tahmasebi Ghorabi S, Faghih R, Behzadi A, Aryan A. Effect of Methamphetamine on Human Spatial Arrangement in Testicular Cells. Iranian Journal of Toxicology. 2026; 160-166. doi: 10.22034/IJT.20.3.160

doi: 10.22034/IJT.20.3.160

Article info
Received: June 09, 2026
Accepted: July 13, 2026
Online Published: July 19, 2026

*** Corresponding author:**
Arefeh Aryan, Department of Anatomical Sciences, Lorestan University of Medical Sciences, Khorramabad, Iran

E-mail: arefeharyan@gmail.com

ABSTRACT

Background: Methamphetamine (METH) is a widely abused psychostimulant known primarily for its neurotoxicity. Growing evidence from animal studies reveals substantial testicular toxicity, whereas human data on structural changes remain extremely limited. No previous study has quantitatively evaluated the cytoarchitectural organization of testicular cells in chronic METH users. The present study aimed to investigate the impact of chronic METH exposure on the spatial distribution and territorial organization of human testicular cells through Voronoi tessellation-based quantitative analysis.

Methods: Post-mortem testicular tissue was obtained from 10 chronic METH users (confirmed by toxicology) and 10 age-matched drug-free controls. Sections were imaged at 40× magnification. Voronoi tessellation was performed using Fiji/ImageJ with cell nuclei as seed points. For each case, the coefficient of variation (CV) of Voronoi polygon areas, mean polygon area, and polygon size distribution were measured. Differences between groups were compared using an unpaired two-tailed Student's t-test.

Results: Chronic METH users showed a significantly higher coefficient of variation in Voronoi polygon areas compared to controls (6.73±1.97% vs. 3.68±0.96%; p=0.003), indicating increased spatial irregularity. Polygon size distribution was shifted, with a significantly higher proportion of larger polygons (>131 arbitrary units) in the METH group (18.3% vs. 7.4%; p=0.04). Although mean Voronoi polygon area was slightly reduced in METH users, it showed no statistical significance (122.53±3.09 vs. 123.62±1.91 arbitrary units; p=0.12).

Conclusion: Chronic METH use is associated with statistically significant alterations in the spatial organization of human testicular cells, characterized by increased coefficient of variation and shifted Voronoi polygon size distribution.

Keywords: Human Testis, Methamphetamine, Testicular Toxicity, Spatial Arrangement, Voronoi Tessellation

Introduction

Methamphetamine (METH) is one of the most widely abused amphetamine-type stimulants, particularly among adolescents and young adults of reproductive age, and its global burden continues to rise. While METH is well recognized for its potent neurotoxic properties mediated by excessive dopamine release and impaired reuptake, accumulating evidence indicates that its toxicity extends beyond the central nervous system and affects multiple peripheral organs, including the male reproductive system [1, 2]. The testicular microenvironment appears particularly vulnerable, raising concerns about the potential impact of chronic METH exposure on spermatogenesis and male fertility.

Animal studies consistently demonstrate reductions in body, testicular, and epididymal weights following prolonged METH administration [3]. Methamphetamine administration induces apoptosis in seminiferous tubules, particularly in spermatogonia and primary spermatocytes, and leads to decreased germ cell density. Histological analyses reveal significant epithelial gaps between the spermatogonia and other cell layers due to integrity disruption, and disorganized tubular structure [4-6]. Additionally, METH suppresses Sertoli cell proliferation, impairs mitochondrial function, and increases blood-testis barrier (BTB) permeability, contributing to oxidative stress, inflammation, and disruption of the spatial organization within the seminiferous epithelium [7]. These structural disruptions culminate in impaired spermatogenesis and spermiogenesis [8]. A human forensic autopsy study has demonstrated that METH and

its metabolite amphetamine accumulate in the testes and prostate at median concentrations 3–5 times higher than in peripheral blood, with testicular levels correlating significantly with iliac vein blood but not urine [9].

Human data on METH-induced testicular toxicity are extremely limited. The autopsy studies only examined drug accumulation, without evaluating morphological or spatial alterations. Moreover, although animal studies have extensively documented testicular toxicity, none has applied quantitative spatial analyses to examine cytoarchitectural organization of germ cells. Consequently, the spatial and structural organization of testicular cells in METH-exposed human tissue remains largely uncharacterized.

Conventional histological evaluations, including Johnsen's scoring, tubular morphology grading, and germ cell layer counting, provide valuable qualitative insights but fail to quantify the precise spatial relationships between cells within the seminiferous niche. Given that efficient spermatogenesis requires coordinated positioning of germ cells and Sertoli cells, methods that can capture subtle cytoarchitectural alterations are needed. Voronoi tessellation offers an advanced quantitative approach by partitioning tissue into polygonal regions centered on individual nuclei, enabling measurement of local cell density, nearest-neighbor relationships, and deviations from regular, random, or clustered spatial patterns. This technique is particularly well-suited for detecting microarchitectural disturbances that may be overlooked by qualitative assessments [10, 11].

Therefore, the present research aimed to apply Voronoi tessellation to post-mortem human testicular tissue from chronic METH users and age-matched controls to quantitatively characterize alterations in cell spatial distribution and Voronoi polygon areas. This analysis seeks to reveal cytoarchitectural disruptions associated with chronic METH exposure that cannot be captured through conventional histopathological methods.

Materials and Methods

Study Design and Sample Collection

This retrospective case-control analysis aimed to investigate the impact of chronic METH use on the spatial arrangement of human testicular cells using Voronoi tessellation. Testicular specimens were obtained post-mortem from 10 individuals with confirmed METH use (case group) and 10 age-matched healthy individuals (control group) by the Forensic Medicine Organization of Iran. Inclusion criteria for the case group included individuals aged 25–45 years with a history of METH consumption confirmed by toxicological testing, no concurrent use of other drugs or toxins, and absence of genital disorders or infertility. The control group comprised individuals aged 33–38 years who died from non-drug-related causes, such as electric shock, accident, or carbon monoxide poisoning, with no history of disease or reproductive issues. Cases with positive tests for other substances (e.g., hemp, tramadol, morphine, or methadone) or confounding medical histories were excluded.

Post-mortem sampling was carried out 8–10 h after death, with family consent obtained. Tissue samples measuring 3 × 3 cm² were excised via incisional autopsy for histological evaluation. Methamphetamine use was verified using a multi-step toxicological protocol: [1] rapid urine testing with a 12-drug diagnostic kit; [2] high-performance liquid chromatography (HPLC); and [3] gas chromatography–mass spectrometry (GC/MS). Samples from liver tissue, gastric contents, bile, urine, and vitreous fluid were analyzed for acidic, alkaline, and opioid drugs. Positive preliminary results via thin-layer chromatography (TLC) prompted further HPLC and GC/MS confirmation. Amphetamines were derivatized with heptafluorobutyric anhydride (HFBA) for GC/MS identification. Headspace GC analysis of blood and vitreous samples ruled out volatile substances. All analyses were performed blindly to ensure objectivity.

Voronoi Tessellation Analysis

Testicular tissue sections were processed for Voronoi tessellation to quantify the spatial distribution of cells. Ten tissue sections per sample were imaged using a video-microscopy system with a 40× objective lens. The nucleus of each testicular cell served as the seed point for tessellation. Analysis was conducted using Fiji ImageJ software (National Institutes of Health, USA) following these steps: (A) Import the microscopic image and a 40× scale bar image (e.g., 50 µm=241 pixels). (B) Set the scale under the "Analyze" menu. (C) Under "Plugins > Analyze," select "Voronoi tessellation." (D) Use the "Multipoint" tool to mark cell nuclei. (E) Generate and screenshot the Voronoi polygons, then re-import the screenshot. (F) Convert to 8-bit grayscale under "Image > Type." (G) Adjust threshold under "Image > Adjust" to isolate polygons (black on white background). (H) Use the "Wand" tracing tool to select polygons and measure area, perimeter, mean, and standard deviation (SD) via right-click "Measure."

Polygon area variability was assessed using the coefficient of variation (CV), calculated as CV = (SD/mean) × 100. Spatial patterns were classified as follows: CV < 33% indicated regular distribution; 33.1–64% indicated random arrangement; and >64% indicated clustered distribution. Mean polygon areas were categorized into bins (>120, 121–130, >131) to evaluate percentage distributions between groups.

Data Analysis

Raw data on CV and mean polygon areas were collected from 10 samples per group. Percentage distributions of Voronoi polygon areas were derived from aggregated measurements. Statistical analysis was performed using an unpaired two-tailed Student's t-test to compare CV and mean polygon areas between groups. A P-value < 0.05 was considered statistically significant.

The collected data were visualized using bar graphs with error bars representing SD, generated with Fiji ImageJ and exported as figures.

Results

Sample Characteristics

Table 1 summarizes the demographic and clinical profiles of the 10 METH users and 10 controls. Methamphetamine users had a mean age of 35.3 years (range: 33–38 years), with consumption durations of 5–6 years and sampling times post-death of 7–13 h. Causes of death included overdose (n=4), cardiac arrest (n=2), drowning following high METH intake (n=1), brain hemorrhage following excessive METH consumption (n=1), apnea (n=1), and advanced respiratory infection following long-term METH use (n=1). Routes of administration were primarily intravenous (IV) or IV-smoke combinations. Body mass index (BMI) ranged from 16.8–19.4. One user had a history of suicide, and dental patterns indicated healthy use in most cases. Controls had a mean age of 35.1 years (range: 33–37 years), with causes of death including accident (n=3), myocardial infarction (n=4), carbon monoxide poisoning (n=1), and electric shock (n=1). The BMI ranged from 19.8–31.9, with no drug history or suicide records.

Table 1. Demographic and clinical characteristics of methamphetamine users and reference (control) group

Sample number	Sampling time after death (h)	Duration of consumption of met (year)	BMI	The ultimate cause of death	Age	Suicide history	The type of use met	Healthy dental pattern
Met 1	7	5	18.2	Advanced respiratory infection following long-term Meth consumption	33	-	IV-S	16
Met 2	10	5	17.4	Cardiac arrest	34	1	IV	20
Met 3	10	5	17.9	Overdose	38	-	IV	16
Met 4	11	5	17	Cardiac arrest	37	-	S	22
Met 5	11	6	17.2	Overdose	36	2	IV-S	24
Met 6	12	5	16.8	Apnoea	35	-	IV-S	13
Met 7	13	5	19.2	Overdose	34	1	IV-O	19
Met 8	8	6	19.4	Brain haemorrhage following excessive Meth consumption	38	-	IV	24
Met 9	10	5	18.9	Drowning following high Meth intake	36	-	IV-S	27
Met 10	13	5	17.4	Overdose	36	1	IV-S	23
Ref 1	7	-	20.8	Accident	38	-	-	30
Ref 2	9	-	21.9	Carbon monoxide poisoning	37	-	-	28
Ref 3	11	-	26.3	Myocardial infarction	37	-	-	28
Ref 4	10	-	23.7	Myocardial infarction	36	-	-	26
Ref 5	12	-	30.2	Accident	38	-	-	29
Ref 6	8	-	21.9	Myocardial infarction	37	-	-	30
Ref 7	9	-	26.4	Accident	33	-	-	29
Ref 8	10	-	22.4	Electric shock	35	-	-	29
Ref 9	8	-	30.7	Myocardial infarction	34	-	-	26
Ref 10	9	-	19.8	Myocardial infarction	36	-	-	30

Coefficient of Variation in Voronoi Polygon Areas

The CV of Voronoi polygon areas, reflecting spatial variability in testicular cell arrangement, was significantly higher in the METH group compared to controls (Figure 1, p=0.003). Mean CV was 3.68% ± 0.96% (SD) in controls and 6.73% ± 1.97% in METH users, indicating greater heterogeneity in cell distribution among users. All CV values remained below 33% (control range: 2.37–5.64%; METH range: 4.12–10.54%), consistent with a regular spatial pattern in both groups. The elevated CV in the METH group suggests subtle disruptions in cellular uniformity.

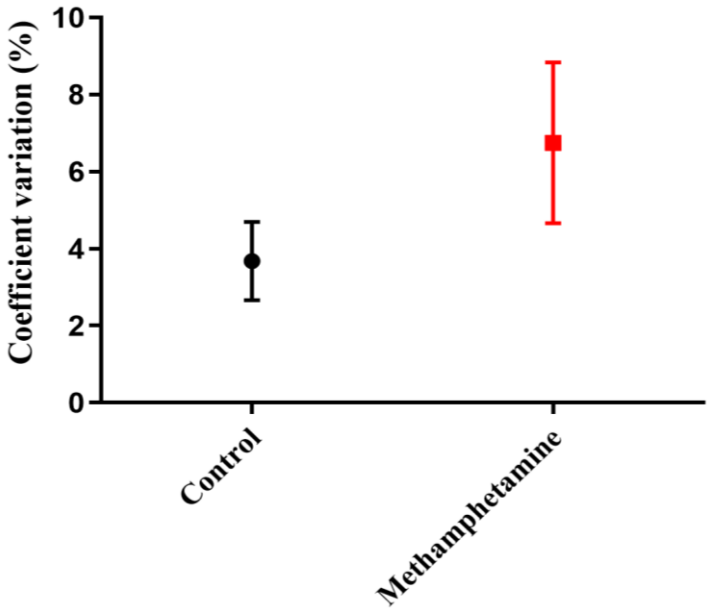

Figure 1. Comparison of the Coefficient of Variation (CV) in Voronoi polygon areas between the Control and Methamphetamine groups. The error bars represent the standard deviation (SD)

Mean Area of Voronoi Polygons

Mean Voronoi polygon areas, representing the average territorial space per testicular cell, showed a slight reduction in the METH group, though not statistically significant (Fig. 2, p=0.12). Controls showed a mean area of 123.62 ± 1.91 arbitrary units, compared with 122.53 ± 3.09 arbitrary units in METH users. Although this minor difference may imply subtle cellular compaction, the overlap in values indicates no major structural alteration.

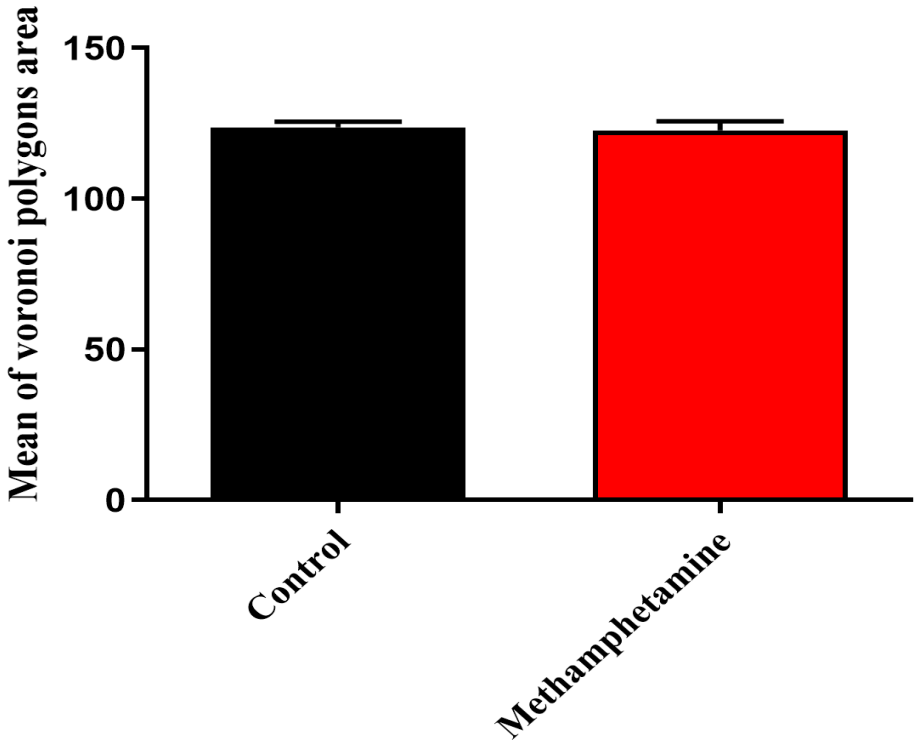

Figure 2. Mean Voronoi polygon areas in the control and methamphetamine groups

Percentage Distribution of Voronoi Polygon Areas

The distribution of Voronoi polygon areas across size categories revealed shifts in the METH group (Fig. 3). In controls, 63.1% of polygons fell in the 121–130 range, 30.1% were >120, and 7.4% were >131. In contrast, METH users showed 41.0% in the 121–130 range, 41.0% >120, and 18.3% >131. This shift indicates a higher proportion of smaller (>120) and larger (>131) polygons in users, supporting increased spatial irregularity (p=0.04

for >131 category comparison).

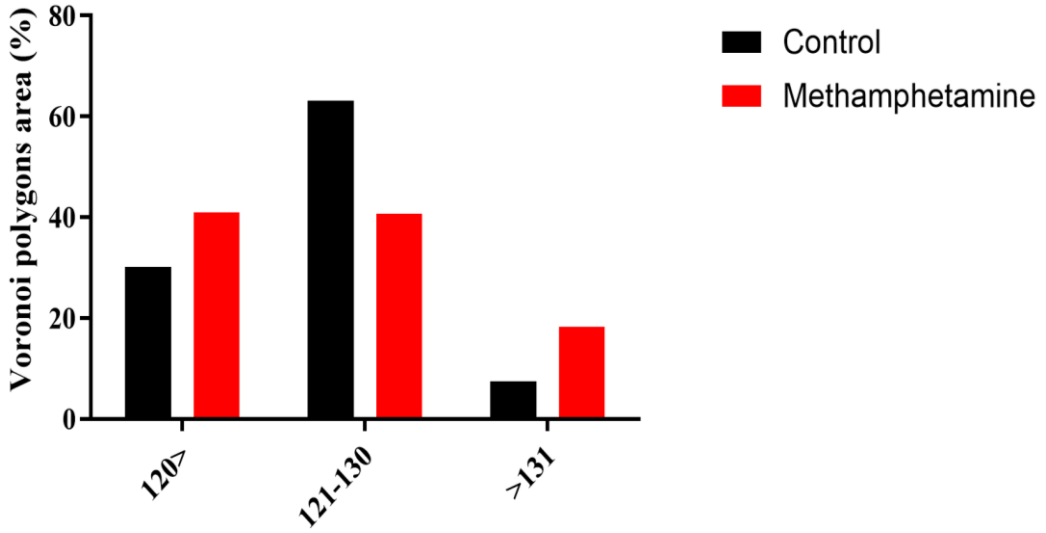

Figure 3. Percentage distribution of Voronoi polygon areas across different size categories (<120, 121–130, and >131) for control and methamphetamine groups

Morphometric Findings

Quantitative morphometric analysis via Voronoi tessellation revealed a significant disruption in the spatial organization of testicular cells in the METH group compared to the control group (Fig. 4). The control group exhibited a predominantly regular cellular distribution, with CV < 33%, consistent with healthy testicular architecture. In contrast, the METH-exposed group showed a significant increase in polygon area variability, with CV values shifting toward the clustered distribution range (CV>64%). As illustrated in Fig. 4B, D, F, the Voronoi polygons in the METH group were highly irregular in size and shape, indicating a transition from a homeostatic state to a disorganized, clustered cellular arrangement. Statistical analysis confirmed that the mean polygon area and the CV were significantly different between the two groups (p<0.05).

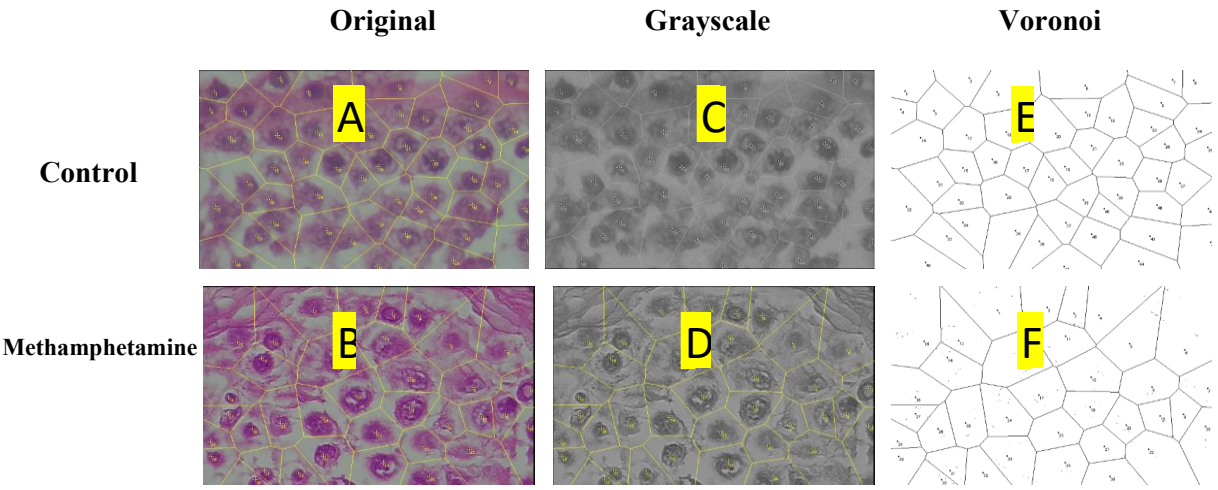

Figure 4. Voronoi tessellation analysis of testicular tissue architecture. (A, C, E) Representative images from the **control group**, exhibiting a highly organized and uniform cellular distribution. (B, D, F) Representative images from the **METH-treated group**, demonstrating increased heterogeneity in polygon size and shape, indicative of disrupted cellular spatial arrangement. Columns display: (A, B) Original H&E-stained sections; (C, D) Scaled images with overlaid tessellation; and (E, F) Final binary output of Voronoi polygons used for quantification.

Discussion

The present quantitative analysis revealed a shifted distribution of Voronoi polygon sizes in METH users, characterized by a higher proportion of both smaller and larger polygons, a bidirectional deviation that supports increased spatial irregularity compared to controls (significant in the >131 category, p=0.04). This irregularity is further corroborated by greater heterogeneity in cell distribution among METH users, with a Mean CV of 6.73% ± 1.97% versus 3.68% ± 0.96% in controls. Despite this, the mean area of Voronoi polygons was not significantly higher in users (122.53±3.09) compared to controls (123.62±1.91,

p=0.12), suggesting minor cellular compaction without major structural alteration.

Animal studies have consistently reported significant METH-induced testicular toxicity. Chronic administration leads to reduced testicular and epididymal weights and induces marked apoptosis within the seminiferous epithelium, particularly affecting spermatogonia and primary spermatocytes [3, 4]. Histological disruptions include widening of epithelial gaps, decreased germ-cell density, and disorganization of tubular architecture [5, 6, 12]. These findings collectively demonstrate that METH alters both cellular integrity and the structural coordination of the seminiferous tubules, forming a mechanistic basis for impaired spermatogenesis. These changes may be driven by several mechanisms besides the mentioned ones, including impaired Sertoli cell function and BTB integrity, oxidative stress, and inflammation, all of which could subtly disrupt the spatial organization of testicular cells [7, 8].

Compared with the extensive testicular damage documented in experimental models, the findings of the present study demonstrate only subtle alterations in human samples. Mean Voronoi polygon area showed a nominal, non-significant reduction in METH users compared with controls. The coefficient of variation increased significantly, yet remained within the “regular pattern” range, indicating mild irregularity. Polygon size distribution was more heterogeneous in METH users, reflecting localized microarchitectural disturbance rather than widespread disorganization.

These findings suggest that the spatial alterations in human testes follow a pattern likely similar to that observed in animal studies, reflecting mild irregularity rather than extensive damage. However, the overall severity in humans is lower, and widespread disruption of seminiferous architecture is absent. This milder effect may be attributed to differences in METH exposure, dosing, or inherent tissue resilience.

To date, only one human autopsy study has shown METH accumulation in the testes, without examining tissue structure or cell arrangement [9]. The present study provides quantitative evidence of mild testicular spatial irregularity in humans, paralleling animal findings but with lower severity, and demonstrates the utility of Voronoi tessellation for future analyses.

To our knowledge, the current research is the first quantitative analysis of human testicular tissue from chronic METH users, using Voronoi tessellation as an objective method. Age-matched controls and standardized post-mortem sampling strengthen the reliability of the findings. However, the sample size was small (n=10 per group), and detailed METH dose was unavailable. Only post-mortem tissue was analyzed, which may be influenced by death-related changes.

Conclusions

In conclusion, chronic METH exposure is associated with mild alterations in the spatial organization of human testicular cells, evidenced by increased CV and subtle shifts in Voronoi polygon distributions, while overall cell territory (mean area) remains largely unchanged. These findings provide quantitative human evidence of testicular cytoarchitectural changes under METH exposure, bridging gaps left by prior animal and autopsy studies. Future research with larger cohorts and functional assessments of spermatogenesis is warranted to further elucidate the impact of chronic METH use on male fertility.

Conflicts of Interest

The authors declare that there is no conflict of interest regarding the publication of this study.

Funding

This research received no external funding from public, commercial, or not-for-profit organizations.

Compliance with Ethical Guidelines

This study was conducted in accordance with the ethical principles of biomedical research. Ethical approval for the study was obtained from the Ethics Committee of Shiraz University of Medical Sciences, Shiraz, Iran (Ethics Code: IR.SUMS.REC.1399.820).

Authors' Contributions

A.K.R methodology, data analysis, and interpretation of results. S.T. Gh and R.F article structuring and writing.

A.A revision and supervision. A.B and A.A analysis and scoring of the kidney damages. All authors have read and approved the manuscript prior to submission for publication.

Data Access and Responsibility

The authors confirm that all the data supporting the findings of this study are available within the article. All authors had full access to the data and take responsibility for the integrity and accuracy of the data analysis.

List of abbreviations

METH = Methamphetamine
BTB = Blood-testis barrier
CV = Coefficient of variation
SD = Standard deviation
GC/MS = Gas chromatography–mass spectrometry
HPLC = High-performance liquid chromatography
TLC = Thin-layer chromatography
HFBA = Heptafluorobutyric anhydride
BMI = Body mass index
IV = Intravenous

References

1. Allaeian Jahromi Z, Meshkibaf MH, Naghdi M, Vahdati A, Makoolati Z. Methamphetamine downregulates the sperm-specific calcium channels involved in sperm motility in rats. ACS Omega. 2022;**7**(6):5190-6. [DOI: 10.1021/acsomega.1c06242] [PMID: 35187334] [PMCID: PMC8851642]
2. Liu J-L, Chen L-J, Liu Y, Li J-H, Zhang K-K, Hsu C, et al. The gut microbiota contributes to methamphetamine-induced reproductive toxicity in male mice. Ecotoxicol Environ Saf. 2024;**279**:116457. [DOI: 10.1016/j.ecoenv.2024.116457] [PMID: 38754198]
3. Lin J-F, Lin Y-H, Liao P-C, Lin Y-C, Tsai T-F, Chou K-Y, et al. Induction of testicular damage by daily methamphetamine administration in rats. Chin J Physiol. 2014;**57**(1):19-30. [DOI: 10.4077/CJP.2014.BAB155] [PMID: 24621335]

4. Yamamoto Y, Yamamoto K, Hayase T, Abiru H, Shiota K, Mori C. Methamphetamine induces apoptosis in seminiferous tubules in male mice testis. Toxicol Appl Pharmacol. 2002;**178**:155-60. [DOI: 10.1006/taap.2001.9330] [PMID: 11858731]
5. Alavi SH, Taghavi MM, Moallem SA. Evaluation of effects of methamphetamine repeated dosing on proliferation and apoptosis of rat germ cells. Syst Biol Reprod Med. 2008;**54**(2):85-91. [DOI: 10.1080/19396360801952078.] [PMID:18446649]
6. Saberi A, Sepehri G, Safi Z, Razavi B, Jahandari F, Divsalar K, et al. Effects of methamphetamine on testes histopathology and spermatogenesis indices of adult male rats. Addict Heal. 2017;**9**:199-205. [PMID: 30574282] [PMCID: PMC6294480]
7. Fisher D, Zabida O, Abdul-Rasool S, Willemse C. Cytotoxicity of methamphetamine exposure on Sertoli cells: a pilot study with implications for male infertility. Drug Chem Toxicol. 2025;**48**(6):1317-27. [DOI: 10.1080/01480545.2025.2471383] [PMID: 40034051]
8. Adisa FB, Oyovwi MO, Ajayi AF. Mechanisms underlying methamphetamine-induced disruption of testicular integrity. Naunyn Schmiedebergs Arch Pharmacol. 2025;**398**(12):16461-77. [DOI: 10.1007/s00210-025-04311-8] [PMID: 40600989]
9. Tani N, Oritani S, Ono M, Ishikawa T. Forensic significance of quantitatively analyzing methamphetamine in male reproductive organs. Leg Med (Tokyo). 2025;**75**:102618. [DOI: 10.1016/j.legalmed.2025.102618] [PMID: 40252596]
10. Duyckaerts C, Godefroy G. Voronoi tessellation to study the numerical density and the spatial distribution of neurones. J Chem Neuroanat. 2000;**20**:83-92. [DOI: 10.1016/s0891-0618(00)00064-8] [PMID: 11074346]
11. Bock M, Tyagi AK, Kreft J-U, Alt W. Generalized Voronoi tessellation as a model of two-dimensional cell tissue dynamics. Bull Math Biol. 2010;**72**:1696-731. [DOI: 10.1007/s11538-009-9498-3] [PMID: 20082148]
12. Azizi S, Kheirandish R, Dabiri S, Lakzaee M. Adverse effects of methamphetamine on vital organs of male rats: histopathological and immunohistochemical investigations. Iran J Basic Med Sci. 2023;**26**(5):549-57. [DOI: 10.22038/IJBMS.2023.68573.15055] [PMID: 37051094] [PMCID: PMC10083837]